Abundance of primordial black holes in peak theory for an arbitrary power spectrum

Chul-Moon Yoo[1,*], Tomohiro Harada[2], Shin'ichi Hirano[1], and Kazunori Kohri[3,4,5]

[1]*Division of Particle and Astrophysical Science, Graduate School of Science, Nagoya University, Nagoya 464-8602, Japan*
[2]*Department of Physics, Rikkyo University, Toshima, Tokyo 171-8501, Japan*
[3]*Institute of Particle and Nuclear Studies, KEK, 1-1 Oho, Tsukuba, Ibaraki 305-0801, Japan*
[4]*The Graduate University for Advanced Studies (SOKENDAI), 1-1 Oho, Tsukuba, Ibaraki 305-0801, Japan*
[5]*Kavli Institute for the Physics and Mathematics of the Universe (WPI), University of Tokyo, Kashiwa 277-8583, Japan*
[*]E-mail: yoo@gravity.phys.nagoya-u.ac.jp

....
We modify the procedure for estimating the primordial black hole (PBH) abundance proposed in [C.-M. Yoo, T. Harada, J. Garriga, and K. Kohri, Prog. Theor. Exp. Phys. **2018**, 123E01 (2018)] so that it can be applied to a broad power spectrum such as the scale-invariant flat power spectrum. In the new procedure we focus on peaks of the Laplacian of the curvature perturbation $\Delta\zeta$, and use the values of $\Delta\zeta$ and $\Delta\Delta\zeta$ at each peak to specify the profile of ζ as a function of the radial coordinate; the values of ζ and $\Delta\zeta$ are used in the previous paper. The new procedure decouples the larger-scale environmental effect from the estimate of PBH abundance. Because the redundant variance due to the environmental effect is eliminated, we obtain a narrower shape of the mass spectrum compared to the previous procedure. Furthermore, the new procedure allows us to estimate the PBH abundance for the scale-invariant flat power spectrum by introducing a window function. Although the final result depends on the choice of the window function, we show that the k-space tophat window minimizes the extra reduction of the mass spectrum due to the window function. That is, the k-space tophat window has the minimum required property in the theoretical PBH estimation. Our procedure makes it possible to calculate the PBH mass spectrum for an arbitrary power spectrum by using a plausible PBH formation criterion with the nonlinear relation taken into account.
....
Subject Index   E01, E31, E80

1. Introduction

Since Zel'dovich, Novikov, and Hawking pointed out the possibility [1,2], primordial black holes (PBHs) have continued to attract attention. They are still viable candidates for a substantial part of dark matter (see, e.g., Refs. [3,4] and references therein), and a possible origin of the observed binary black holes [5,6]. The mass, spin, or spatial distribution of PBHs provides valuable information about relatively small-scale inhomogeneity in the early universe. When we connect a PBH production scenario and observational constraints on it, theoretical estimation of the PBH distribution is inevitable. Here, we provide a plausible procedure to calculate the PBH mass spectrum for an arbitrary power spectrum based on the peak theory.

   Until relatively recently, the Press–Schechter (PS) formalism was applied to the estimation of PBH abundance, based on a perturbation variable such as the comoving density or the curvature perturbation. As PBHs started to draw more attention after the discovery of the binary black holes, as

well as gravitational waves, people have begun to seriously doubt the relevance of the PS formalism in the estimation of PBH abundance. In order to improve the estimation, one needs to resolve the following mutually related issues: the PBH formation criterion, the statistical treatment of nonlinear variables [7], and the use of a window function [8–10].

For the criterion of PBH formation, there has been a long-term debate since Carr proposed a rough criterion [11]. A lot of efforts to clarify the appropriate criterion have been made through numerical and analytic treatments [12–21]. One useful criterion was proposed in Ref. [14] by using the compaction function, which is equivalent to half of the volume average of the density perturbation in the long-wavelength limit [22]. In Ref. [22], through spherically symmetric numerical simulations, it was shown that the threshold of the maximum value of the compaction function gives a relatively accurate criterion which is within about 10% accuracy for a moderate shape of initial configuration. More recently, the threshold value for the volume average of the compaction function was proposed in Ref. [23], and it was shown that this variable gives the PBH formation criterion within 2% accuracy for a moderate inhomogeneity in the radiation-dominated universe (see Ref. [24] for general cosmological background). These recent developments show that the use of the compaction function is crucial for an accurate estimation of PBH abundance.

Another important ingredient in the calculation of PBH abundance is the statistics of perturbation variables. Naively, we would expect the curvature perturbation to be relevant for the Gaussian distribution assumed in the PS formalism. However, the absolute value of the curvature perturbation does not have any physical meaning in a local sense because it can be absorbed into the coordinate rescaling. Therefore, setting the threshold value for the absolute value of the curvature perturbation seems irrelevant. Conversely, while setting the threshold on the compaction function would be appropriate, the compaction function cannot be a Gaussian variable even if the curvature perturbation is totally Gaussian because of their nonlinear relation. Furthermore, the difference in the gauge confuses the relation between perturbation variables.

In Ref. [22], the relations between different gauge conditions were summarized and the gauge issue clarified. The compaction function is expressed in terms of the curvature perturbation in the same reference [22]. Then, apart from the window function, the remaining issue is how to count the number of PBHs by taking into account the nonlinear relation between the curvature perturbation and the compaction function. Although a few procedures for treating the nonlinear relation have been proposed [25,26], their consistency with each other is not yet clear.

In Ref. [25], a plausible procedure to estimate PBH abundance for a narrow power spectrum of the Gaussian curvature perturbation was proposed, where the threshold for the compaction function is used and the nonlinear relation is taken into account. However, this procedure cannot be directly applied to a broad spectrum (see Ref. [27] for a simple approach with linear relations). Our aim in this paper is to improve the procedure in Ref. [25] so that we can introduce a window function, and make it possible to apply to any power spectrum.

The paper is organized as follows. First, the criterion based on the compaction function is introduced in Sect. 2. In Sect. 3, focusing on a high peak of the Laplacian of the curvature perturbation $\Delta\zeta$, we characterize the typical profile of the curvature perturbation ζ around the peak by using the values of $\Delta\zeta$ and $\Delta\Delta\zeta$. This treatment allows us to decouple the environmental effect on the absolute value of the curvature perturbation, and the criterion can be expressed in a purely local manner. In Sect. 4, the procedure to estimate PBH abundance is explained, and applied to the single-scale narrow power spectrum previously presented in Ref. [25]. We discuss the case of the scale-invariant flat spectrum implementing a window function in Sect. 5. Section 6 is devoted to a summary and discussion.

Throughout this paper we use geometrized units in which both the speed of light and Newton's gravitational constant are unity, $c = G = 1$.

2. Criterion for PBH formation

Let us consider the spatial metric given by

$$ds_3^2 = a^2 e^{-2\zeta} \tilde{\gamma}_{ij} dx^i dx^j, \tag{1}$$

with $\det \tilde{\gamma}$ being the same as the determinant of the reference flat metric, where a and ζ are the scale factor of the background universe and the curvature perturbation, respectively. In the long-wavelength approximation, the curvature perturbation ζ and the density perturbation δ with the comoving slicing are related by [22]

$$\delta = -\frac{8}{9} \frac{1}{a^2 H^2} e^{5\zeta/2} \Delta \left(e^{-\zeta/2} \right) \tag{2}$$

in the radiation-dominated universe, where H is the Hubble expansion rate and Δ is the Laplacian of the reference flat metric.

We will be interested mainly in high peaks, which tend to be nearly spherically symmetric [28]. Therefore, in this section we introduce the criterion for PBH formation originally proposed in Ref. [14] assuming spherical symmetry. Here, we basically follow and refer to the discussions and calculation in Ref. [22].

First, let us define the compaction function $\mathcal{C}$ as

$$\mathcal{C} := \frac{\delta M}{R}, \tag{3}$$

where R is the areal radius at the radius r, and δM is the excess of the Misner–Sharp mass enclosed by the sphere of radius r compared with the mass inside the sphere in the fiducial flat Friedmann–Lemaître–Robertson–Walker universe with the same areal radius. From the definition of $\mathcal{C}$, we can derive the following simple form in the comoving slicing (see also Eq. (6.33) in Ref. [22]):

$$\mathcal{C}(r) = \frac{1}{3} \left[1 - \left(1 - r\zeta' \right)^2 \right]. \tag{4}$$

We will assume that the function $\mathcal{C}$ is a smooth function of r for $r > 0$. Then, the value of $\mathcal{C}$ takes the maximum value $\mathcal{C}^{\mathrm{max}}$ at r_{m}, which satisfies

$$\mathcal{C}'(r_{\mathrm{m}}) = 0 \Leftrightarrow \left(\zeta' + r\zeta'' \right) |_{r=r_{\mathrm{m}}} = 0. \tag{5}$$

We consider the following criterion for PBH formation:

$$\mathcal{C}^{\mathrm{max}} > \mathcal{C}_{\mathrm{th}} \equiv \frac{1}{2} \delta_{\mathrm{th}}. \tag{6}$$

In the comoving slicing, the threshold $\mathcal{C}_{\mathrm{th}}$ for PBH formation is evaluated as $\simeq 0.267$ (see Figs. 2 and 3 or Tables I and II in Ref. [22]). This threshold corresponds to the perturbation profiles of Refs. [14,17,29], and is found to be quite robust for a broad range of parameters (see Ref. [23] for a more robust criterion). In this paper we shall use this value as a reference value.

3.   Peak of $\Delta\zeta$ and the spherical profile

Throughout this paper we assume the random Gaussian distribution of ζ with its power spectrum $\mathcal{P}(k)$ defined by the following equation:

$$\langle \tilde{\zeta}^*(\boldsymbol{k})\tilde{\zeta}(\boldsymbol{k}')\rangle = \frac{2\pi^2}{k^3}\mathcal{P}(k)(2\pi)^3\delta(\boldsymbol{k}-\boldsymbol{k}'), \tag{7}$$

where $\tilde{\zeta}(\boldsymbol{k})$ is the Fourier transform of ζ and the bracket $\langle\ldots\rangle$ denotes the ensemble average. Each gradient moment σ_n can be calculated by

$$\sigma_n^2 := \int \frac{dk}{k} k^{2n}\mathcal{P}(k). \tag{8}$$

Hereafter we suppose that the power spectrum is given. Then the gradient moments can be calculated from the power spectrum and regarded as constants.

   In this paper we focus on high peaks of $\zeta_2 := \Delta\zeta$, which coincide with peaks of δ with a linear relation. We note that this procedure is different from the previous one proposed in Ref. [25], where peaks of $-\zeta$ were considered.

   Focusing on a high peak of ζ_2 and taking it as the origin of the coordinates, we introduce the amplitude μ_2 and the curvature scale $1/k_\bullet$ of the peak as follows:[1]

$$\mu_2 = \zeta_2|_{r=0}, \tag{9}$$

$$k_\bullet^2 = -\frac{\Delta\Delta\zeta|_{r=0}}{\mu_2}. \tag{10}$$

According to the peak theory [28], for a high peak, assuming spherical symmetry, we may expect the typical form of the profile $\bar{\zeta}_2$ to be described using μ_2 and $k_\bullet$ as follows:

$$\frac{\bar{\zeta}_2(r)}{\sigma_2} = \frac{\mu_2/\sigma_2}{1-\gamma_3^2}\left(\psi_2 + \frac{1}{3}R_\bullet^2\Delta\psi_2\right) - \frac{\mu_2 k_\bullet^2/\sigma_4}{\gamma_3(1-\gamma_3^2)}\left(\gamma_3^2\psi_2 + \frac{1}{3}R_\bullet^2\Delta\psi_2\right), \tag{11}$$

with $\gamma_3 = \sigma_3^2/(\sigma_2\sigma_4)$, $R_\bullet = \sqrt{3}\sigma_3/\sigma_4$, and

$$\psi_n(r) = \frac{1}{\sigma_2^2}\int \frac{dk}{k} k^{2n}\frac{\sin(kr)}{kr}\mathcal{P}(k). \tag{12}$$

It is worth noting that for $k_\bullet = \sigma_3/\sigma_2$ we obtain

$$\bar{\zeta}_2(r;\sigma_3/\sigma_2) = \mu_2\psi_2(r). \tag{13}$$

It will be shown in Eq. (27) that, regarding $k_\bullet$ as a probability variable, we obtain σ_3/σ_2 as the mean value of $k_\bullet$.

   Let us consider the profile $\bar{\zeta}$ given by integrating Eq. (11). Integrating $\bar{\zeta}_2$, and assuming regularity at the center, we obtain

$$\frac{\bar{\zeta}(r)}{\sigma_2} = -\frac{\mu_2/\sigma_2}{(1-\gamma_3^2)}\left(\psi_1 + \frac{1}{3}R_\bullet\Delta\psi_1\right) + \frac{\mu_2 k_\bullet^2/\sigma_4}{\gamma_3(1-\gamma_3^2)}\left(\gamma_3^2\psi_1 + \frac{1}{3}R_\bullet\Delta\psi_1\right) + \frac{\zeta_\infty}{\sigma_2}, \tag{14}$$

---

[1] The notation of the amplitude μ_2 and the curvature scale $k_\bullet$ are chosen so that they will be distinguished from μ and k_* in Ref. [25].

where $\zeta_\infty = \bar{\zeta}|_{r=\infty}$ is an integration constant. Because we have $\psi_1|_{r=0} = \sigma_1^2/\sigma_2^2$ and $\Delta\psi_1|_{r=0} = -1$, we obtain

$$\zeta_0 := \bar{\zeta}|_{r=0} = -\mu_2 \frac{\sigma_1^2\sigma_4^2 - \sigma_2^2\sigma_3^2 + (\sigma_2^4 - \sigma_1^2\sigma_3^2)k_\bullet^2}{\sigma_2^2\sigma_4^2 - \sigma_3^4} + \zeta_\infty. \tag{15}$$

We may consider either ζ_0 or ζ_∞ as a probability variable. Since the constant shift of ζ can be absorbed into the renormalization of the background scale factor, a nonzero value of ζ_∞ would be regarded as a larger-scale environmental effect. Actually, in Appendix A we show that the mean value of ζ_∞ is 0 for a given set of μ_2 and $k_\bullet$. In Ref. [25], we used ζ_0 to characterize the profile of the curvature perturbation. However, using ζ_0 would mix the environmental effect with the local state. Therefore, in this paper we ignore ζ_∞ by renormalizing the background scale factor as $e^{-\zeta_\infty}a \to a$ to eliminate the environmental effect, and regard ζ_0 as a dependent variable on μ_2 and $k_\bullet$ through Eq. (15) with $\zeta_\infty = 0$.

In order to obtain PBH abundance we can follow the procedure proposed in Ref. [25], replacing μ and k_* by μ_2 and $k_\bullet$. Here, we just copy part of the procedure from Ref. [25] (a flow chart of our procedure can be seen in Ref. [30]). Applying Eq. (4) to $\bar{\zeta}$, we obtain the relation between μ_2 and $\mathcal{C}$ as

$$\mu_2 = \frac{1 - \sqrt{1 - 3\mathcal{C}}}{rg'}, \tag{16}$$

where $g(r; k_\bullet) := \bar{\zeta}/\mu_2$ and the smaller root is taken. Let us define the threshold value $\mu_{2\mathrm{th}}^{(k_\bullet)}$ as

$$\mu_{2\mathrm{th}}^{(k_\bullet)}(k_\bullet) = \frac{1 - \sqrt{1 - 3\mathcal{C}_{\mathrm{th}}}}{\bar{r}_\mathrm{m}(k_\bullet)g_\mathrm{m}'(k_\bullet)}, \tag{17}$$

where $\bar{r}_\mathrm{m}(k_\bullet)$ is the value of r_m for $\zeta = \bar{\zeta}$, and

$$g_\mathrm{m}(k_\bullet) := g(\bar{r}_\mathrm{m}(k_\bullet); k_\bullet). \tag{18}$$

In Eq. (17), we explicitly denote the $k_\bullet$ dependence of $\bar{r}_\mathrm{m}$ and g_m to emphasize it.

In order to express the threshold value as a function of the PBH mass M, let us consider the horizon entry condition:

$$aH = \frac{a}{R(\bar{r}_\mathrm{m})} = \frac{1}{\bar{r}_\mathrm{m}}e^{\mu_2 g_\mathrm{m}}. \tag{19}$$

Since the PBH mass is given by $M = \alpha/(2H)$ with α being a numerical factor, from the horizon entry condition in Eq. (19), the PBH mass M can be expressed as

$$M = \frac{1}{2}\alpha H^{-1} = \frac{1}{2}\alpha a\bar{r}_\mathrm{m}e^{-\mu_2 g_\mathrm{m}} = M_\mathrm{eq}k_\mathrm{eq}^2\bar{r}_\mathrm{m}^2 e^{-2\mu_2 g_\mathrm{m}} =: M^{(\mu_2, k_\bullet)}(\mu_2, k_\bullet), \tag{20}$$

where we have used the fact that $H \propto a^{-2}$ and $a = a_\mathrm{eq}^2 H_\mathrm{eq}\bar{r}_\mathrm{m}e^{-\mu_2 g_\mathrm{m}}$, with a_eq and H_eq being the scale factor and Hubble expansion rate at the matter–radiation equality, and M_eq and k_eq defined by $M_\mathrm{eq} = \alpha H_\mathrm{eq}^{-1}/2$ and $k_\mathrm{eq} = a_\mathrm{eq}H_\mathrm{eq}$, respectively. For simplicity we set $\alpha = 1$ as a fiducial value.[2]

---

[2] In order to take into account the critical behavior [31,32], α should be given by a function of μ_2 and $k_\bullet$ as $\alpha = K(k_\bullet)(\mu_2 - \mu_{2\mathrm{th}}(k_\bullet))^\gamma$ with $\gamma \simeq 0.36$ [15,16,18,29,33–37] and $K(k_\bullet)$ being some function of $k_\bullet$, which would be profile dependent.

Then, we can obtain the threshold value of $\mu_{2\text{th}}^{(M)}(M)$ as a function of M by eliminating $k_\bullet$ from Eqs. (20) and $\mu_2 = \mu_{2\text{th}}^{(k_*)}(k_\bullet)$, and solving it for μ_2. That is, defining $k_\bullet^{\text{th}}(M)$ by the inverse function of $M = M^{(\mu_2,k_\bullet)}(\mu_{2\text{th}}^{(k_\bullet)}(k_\bullet), k_\bullet)$, we obtain the threshold value of $\mu_{2\text{th}}^{(M)}$ for a fixed value of M as

$$\mu_{2\text{th}}^{(M)}(M) := \mu_{2\text{th}}^{(k_\bullet)}(k_\bullet^{\text{th}}(M)). \tag{21}$$

Meanwhile, from Eq. (20) we can describe μ_2 as a function of M and $k_\bullet$ as follows:

$$\mu_2 = \mu^{(M,k_\bullet)}(M, k_\bullet) := -\frac{1}{2g_\text{m}} \ln\left(\frac{1}{k_\text{eq}^2 \bar{r}_\text{m}^2} \frac{M}{M_\text{eq}}\right). \tag{22}$$

The value of μ_2 may be bounded below by $\mu_{2\text{min}}(M)$ for a fixed value of M. Actually, in the specific examples in Sects. 4 and 5, the value of $\mu_{2\text{min}}(M)$ is given as

$$\mu_{2\text{min}} = \mu^{(M,k_\bullet)}(M, 0). \tag{23}$$

Then, for a fixed value of M, the region of μ for PBH formation can be given by

$$\mu_2 > \mu_{2\text{b}} := \max\left\{\mu_{2\text{min}}(M), \mu_{2\text{th}}^{(M)}(M)\right\}. \tag{24}$$

4. PBH abundance

From Ref. [25], we obtain the expression for the peak number density characterized by μ_2 and $k_\bullet$ as

$$n_\text{pk}^{(k_\bullet)}(\mu_2, k_\bullet)d\mu_2 dk_\bullet = \frac{2 \cdot 3^{3/2}}{(2\pi)^{3/2}} \mu_2 k_\bullet \frac{\sigma_4^2}{\sigma_2 \sigma_3^3} f\left(\frac{\mu_2 k_\bullet^2}{\sigma_4}\right) P_1\left(\frac{\mu_2}{\sigma_2}, \frac{\mu_2 k_\bullet^2}{\sigma_4}\right) d\mu_2 dk_\bullet, \tag{25}$$

where

$$\begin{aligned} f(x) = \frac{1}{2}x(x^2 - 3)&\left(\text{erf}\left[\frac{1}{2}\sqrt{\frac{5}{2}}x\right] + \text{erf}\left[\sqrt{\frac{5}{2}}x\right]\right) \\ &+ \sqrt{\frac{2}{5\pi}}\left\{\left(\frac{8}{5} + \frac{31}{4}x^2\right)\exp\left[-\frac{5}{8}x^2\right] + \left(-\frac{8}{5} + \frac{1}{2}x^2\right)\exp\left[-\frac{5}{2}x^2\right]\right\} \end{aligned} \tag{26}$$

and

$$P_1\left(\frac{\mu_2}{\sigma_2}, \frac{\mu_2 k_\bullet^2}{\sigma_4}\right) = \frac{\mu_2 k_\bullet}{\pi \sigma_2 \sigma_4 \sqrt{1 - \gamma_3^2}} \exp\left[-\frac{\mu_2^2}{2\tilde{\sigma}(k_\bullet)^2}\right] \tag{27}$$

with

$$\frac{1}{\tilde{\sigma}^2(k_\bullet)} := \frac{1}{\sigma_2^2} + \frac{1}{\sigma_4^2(1 - \gamma_3^2)}\left(k_\bullet^2 - \frac{\sigma_3^2}{\sigma_2^2}\right)^2. \tag{28}$$

In Eq. (25), the following replacements have been made from Eq. (58) in Ref. [25]:

$$\mu \to \mu_2, \quad k_* \to k_\bullet, \quad \sigma_n \to \sigma_{n+2}, \quad \gamma \to \gamma_3. \tag{29}$$

Since the direct observable is not $k_\bullet$ but the PBH mass M, we further change the variable from $k_\bullet$ to M as follows:

$$n_\text{pk}^{(M)}(\mu_2, M)d\mu_2 dM := n_\text{pk}^{(k_\bullet)}(\mu_2, k_\bullet)d\mu_2 dk_\bullet$$

$$= \frac{3^{3/2}}{(2\pi)^{3/2}} \frac{\sigma_4^2}{\sigma_2 \sigma_3^3} \mu_2 k_\bullet f\left(\frac{\mu_2 k_\bullet^2}{\sigma_4}\right) P_1\left(\frac{\mu_2}{\sigma_2}, \frac{\mu_2 k_\bullet^2}{\sigma_4}\right) \left| \frac{d}{dk_\bullet} \ln \bar{r}_m - \mu_2 \frac{d}{dk_\bullet} g_m \right|^{-1} d\mu_2 d\ln M, \quad (30)$$

where $k_\bullet$ should be regarded as a function of μ_2 and M given by solving Eq. (20) for $k_\bullet$. We note that an extended power spectrum is implicitly assumed in the above expression. In the monochromatic spectrum case, the expression reduces to the same expression in Ref. [25] because $\sigma_n = \sigma$ for $\mathcal{P}(k) = \sigma^2 k_0 \delta(k - k_0)$.

It should be noted that, since we relate $k_\bullet$ to M with μ_2 fixed, we have implicitly assumed that there is only one peak with $\Delta\zeta_2 = -\mu_2 k_\bullet^2$ in the region corresponding to the mass M, that is, inside $r = r_m$. If the spectrum is broad enough or has multiple peaks at far separated scales, and the typical PBH mass is relatively larger than the minimum scale given by the spectrum, we would find multiple peaks inside $r = r_m$. Then, we cannot correctly count the number of peaks in the scale of interest. In order to avoid this difficulty we need to introduce a window function to smooth out the smaller-scale inhomogeneities. We discuss this issue in the subsequent section. In this section we simply assume that the power spectrum is characterized by a single scale k_0 and there is no contribution from the much smaller scales $k \gg k_0$.

The number density of PBHs is given by

$$n_{BH} d\ln M = \left[\int_{\mu_{2b}}^{\infty} d\mu_2 \, n_{pk}^{(M)}(\mu_2, M) \right] M d\ln M. \quad (31)$$

We also note that the scale factor a is a function of M as $a = 2M^{1/2} M_{eq}^{1/2} k_{eq}/\alpha$. Then, the fraction of PBHs to the total density $\beta_0 d\ln M$ can be given by

$$\beta_0 d\ln M = \frac{M n_{BH}}{\rho a^3} d\ln M = \frac{4\pi}{3} \alpha n_{BH} k_{eq}^{-3} \left(\frac{M}{M_{eq}}\right)^{3/2} d\ln M$$

$$= \frac{2 \cdot 3^{1/2} \alpha k_{eq}^{-3}}{(2\pi)^{1/2}} \frac{\sigma_4^2}{\sigma_2 \sigma_3^3} \left(\frac{M}{M_{eq}}\right)^{3/2} \left[\int_{\mu_{2b}}^{\infty} d\mu \mu_2 k_\bullet f\left(\frac{\mu_2 k_\bullet^2}{\sigma_4}\right) \right.$$

$$\left. P_1\left(\frac{\mu_2}{\sigma_2}, \frac{\mu_2 k_\bullet^2}{\sigma_4}\right) \left| \frac{d}{dk_\bullet} \ln \bar{r}_m - \mu_2 \frac{d}{dk_\bullet} g_m \right|^{-1} \right] d\ln M. \quad (32)$$

Here we note again that $k_\bullet$ should be regarded as a function of μ_2 and M. The above formula can be evaluated in principle once the form of the power spectrum is given. A crucial difference of Eq. (32) from Eq. (61) in Ref. [25] is that the expression does not depend on σ_0, which has infrared-log divergence for the flat scale-invariant spectrum. Thus we can consider the PBH mass spectrum for the flat spectrum without introducing an infrared cut-off.[3]

In order to give a simpler approximate form of Eq. (32), we approximately perform the integral with respect to μ as follows:

$$\beta_0 d\ln M \simeq \frac{2 \cdot 3^{1/2} \alpha k_{eq}^{-3}}{(2\pi)^{1/2}} \frac{\sigma_4^2}{\sigma_2 \sigma_3^3} \left(\frac{M}{M_{eq}}\right)^{3/2} \left[\tilde{\sigma}(k_\bullet)^2 k_\bullet f\left(\frac{\mu_2 k_\bullet^2}{\sigma_4}\right) \right.$$

$$\left. P_1\left(\frac{\mu_2}{\sigma_2}, \frac{\mu_2 k_\bullet^2}{\sigma_4}\right) \left| \frac{d}{dk_\bullet} \ln \bar{r}_m - \mu_2 \frac{d}{dk_\bullet} g_m \right|^{-1} \right]_{\mu_2 = \mu_{2b}} d\ln M. \quad (33)$$

---

[3] The PBH fraction to the total density f_0 at the equality time is given by $f_0 = \beta_0 (M_{eq}/M)^{1/2}$. We do not explicitly show the form of f_0 in this paper since the scale dependence can be more easily understood by the form of β_0.

Since P_1 given in Eq. (27) has exponential dependence, we may expect that the value of β_0 is sensitive to the exponent $-\mu_2^2/2\tilde{\sigma}^2$. Therefore, assuming $\mu_{2b} = \mu_{2\text{th}}^{(M)} = \mu_{2\text{th}}^{(k_\bullet)}(k_\bullet^{\text{th}}(M))$, we can roughly estimate the maximum value of β_0 at the top of the mass spectrum by considering the value k_t of $k_\bullet$ which minimizes the value of $\mu_{2\text{th}}^{k_\bullet}(k_\bullet)/\tilde{\sigma}$,[4] namely,[5]

$$k_t := \text{argmin}_{k_\bullet} \left[\mu_{2\text{th}}^{(k_\bullet)}(k_\bullet)/\tilde{\sigma}(k_\bullet) \right]. \tag{34}$$

The value of k_t cannot be given in an analytic form in general, and a numerical procedure to find the value of k_t is needed. We note that the value of k_t is independent of the overall constant factor of the power spectrum, and depends only on the profile of the spectrum. Substituting k_t into $k_\bullet$ in Eq. (33), we obtain the following rough estimate for the maximum value $\beta_{0,\text{max}}$:

$$\beta_{0,\text{max}} \simeq \beta_{0,\text{max}}^{\text{approx}} := \frac{2 \cdot 3^{1/2} \alpha k_{\text{eq}}^{-3}}{(2\pi)^{1/2}} \frac{\sigma_4^2}{\sigma_2 \sigma_3^3} \left(\frac{M_t}{M_{\text{eq}}} \right)^{3/2} \left[\tilde{\sigma}(k_\bullet)^2 k_\bullet f \left(\frac{\mu_2 k_\bullet^2}{\sigma_4} \right) \right.$$
$$\left. P_1 \left(\frac{\mu_2}{\sigma_2}, \frac{\mu_2 k_\bullet^2}{\sigma_4} \right) \left| \frac{d}{dk_\bullet} \ln \bar{r}_m - \mu_2 \frac{d}{dk_\bullet} g_m \right|^{-1} \right]_{k_\bullet = k_t, \ \mu_2 = \mu_{2\text{th}}^{(k_\bullet)}(k_t)}, \tag{35}$$

where $M_t := M^{(\mu_2, k_\bullet)}(\mu_{2\text{th}}^{(k_\bullet)}(k_t), k_t)$. We note that the expression in Eq. (35) gives a better approximation for a smaller value of the amplitude of the power spectrum σ^2, and may have a factor of difference from the actual maximum value for $\sigma \gtrsim 0.1$ due to the mass dependence of the factors other than the exponential part, as can be found in the examples below.

Let us consider the extended power spectrum given by

$$\mathcal{P}(k) = 3\sqrt{\frac{6}{\pi}} \sigma^2 \left(\frac{k}{k_0} \right)^3 \exp \left(-\frac{3}{2} \frac{k^2}{k_0^2} \right). \tag{36}$$

Gradient moments are calculated as

$$\sigma_n^2 = \frac{2^{n+1}}{3^n \sqrt{\pi}} \Gamma \left(\frac{3}{2} + n \right) \sigma^2 k_0^{2n}, \tag{37}$$

where Γ represents the gamma function. The result is shown in Fig. 1. Our new procedure gives a narrower and slightly higher spectrum than that obtained in Ref [25]. This behavior can be understood as the environmental effect induced by the variance of ζ_∞. Although the effect is so small that it could be practically ignored in this example, we successfully decoupled the environmental effect.

5. Implementing a window function

In our new procedure, a window function can be straightforwardly implemented. That is, introducing the UV cut-off scale k_W, instead of Eq. (7) we consider the following power spectrum of ζ:

$$\mathcal{P}_W(k) = \mathcal{P}(k) W(k; k_W)^2, \tag{38}$$

where $W(k; k_W)$ is a window function satisfying $W(k; k_W) \leq 1$ and $W(k; k_W) = 0$ for $k \gg k_W$. Then, following the procedure given in the previous section, we can calculate the PBH abundance

---

[4] Expansion around $k_\bullet = \sigma_3/\sigma_2$ like in Ref. [25] does not work well because of the large $k_\bullet$ dependence of $\mu_{2\text{th}}^{(k_\bullet)}$. That is, the peak of the exponent $-\mu_{2\text{th}}^2/\tilde{\sigma}^2$ significantly deviates from $k_\bullet = \sigma_3/\sigma_2$, and the Taylor expansion is not as effective as in Ref. [25].

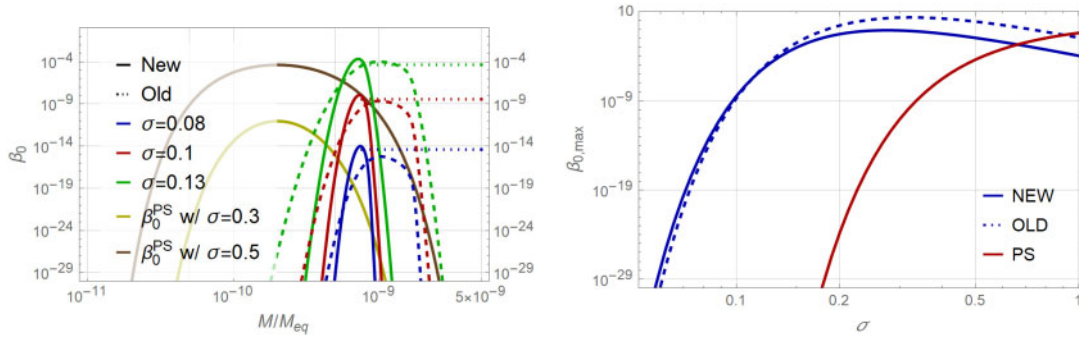[5] $\text{argmin}_x f(x) = \{x \mid \forall y (f(y) \geq f(x))\}$.

Fig. 1. PBH mass spectrum (left) and $\beta_{0,\mathrm{max}}^{\mathrm{approx}}$ as a function of σ (right) for the extended power spectrum in Eq. (36) with $k_0 = 10^5 k_{\mathrm{eq}}$. The solid lines correspond to the spectra calculated by our new procedure with $\alpha = 1$, and the dashed lines show the spectra calculated in Ref. [25]. We also plot the mass spectrum β_0^{PS} obtained from the Press–Schechter formalism explained in Appendix B for comparison. In the left panel, the dotted horizontal lines show the corresponding values of $\beta_{0,\mathrm{max}}^{\mathrm{approx}}$.

for a given value of k_W. The final PBH mass spectrum is given by the envelope curve of the mass spectra for all values of k_W. We note that, for a narrow power spectrum, $\mathcal{P}_W(k) \to \mathcal{P}(k)$ in the limit $k_W \to \infty$, and the mass spectrum results in the case without the window function irrespective of the choice of the window function.

One important issue here is the window function dependence of the final mass spectrum. In order to clarify this issue, let us consider, for a sufficiently broad power spectrum, the effect of the window function for a peak number density at a fixed scale given by the wave number $k_\bullet = k_0$. If $k_0 \gg k_W$, no peak can be found. On the other hand, if $k_0 \ll k_W$, we would find many smaller-scale peaks inside the region of radius $\sim 1/k_0$ because the smaller-scale modes with $k \gg k_0$ are superposed on top of the inhomogeneity with $k \sim k_0$. Thus, every peak has a sharp profile due to the superposed small-scale inhomogeneity and satisfies $k_\bullet \gg k_0$. This means that there is essentially no peak with $k_\bullet = k_0 \ll k_W$ if $k_0 \ll k_W$ and the original power spectrum has a sufficiently broad support in $k > k_0$ (Fig. 2 is an aid to understanding this). For a fixed $k_\bullet = k_0$, in both limits $k_0 \ll k_W$ and $k_0 \gg k_W$ the number of peaks decreases.

In our procedure, since we take the envelope curve for all values of k_W, the final estimate for the peak number density at $k_\bullet = k_0$ is given by the value for k_W which maximizes the peak number density at $k_\bullet = k_0$. For this specific value of k_W, k_0 corresponds to k_{t} introduced in Eq. (35), which basically maximizes the peak number, and generally we have $k_W > k_{\mathrm{t}} \simeq k_0$. If the window function reduces the amplitude of the power spectrum in the region of k much smaller than k_W, the maximum number density of peaks with $k_\bullet = k_0 \simeq k_{\mathrm{t}} < k_W$ also inevitably decreases due to the window function. Thus, the final estimate for the peak number density at $k_\bullet = k_0$ also decreases. For this reason, we expect that a sharp cut-off of the window function would provide a larger value of the peak number density, minimizing the extra reduction of the mass spectrum due to the window function.

Let us check the above discussion by considering the flat scale-invariant spectrum with a window function:

$$\mathcal{P}_W(k; k_W) = \sigma^2 W(k; k_W)^2. \tag{39}$$

We consider the following window functions:

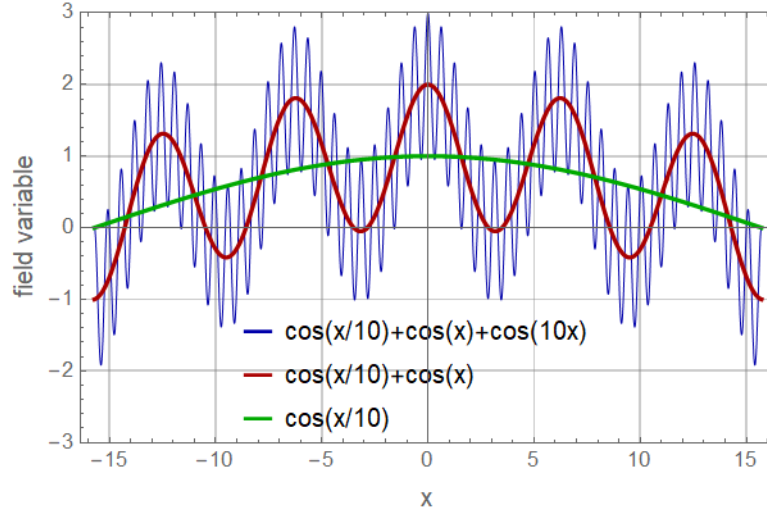$$W_n(k/k_W) = \exp\left(-\frac{1}{2}\frac{k^{2n}}{k_W^{2n}}\right), \tag{40}$$

Fig. 2. Three functions, $\cos(x/10) + \cos(x) + \cos(10x)$, $\cos(x/10) + \cos(x)$, and $\cos(x/10)$, are plotted as functions of x. For $\cos(x/10) + \cos(x)$, every peak has a scale of order 1, but the peak profiles are sharper for $\cos(x/10) + \cos(x) + \cos(10x)$ and broader for $\cos(x/10)$.
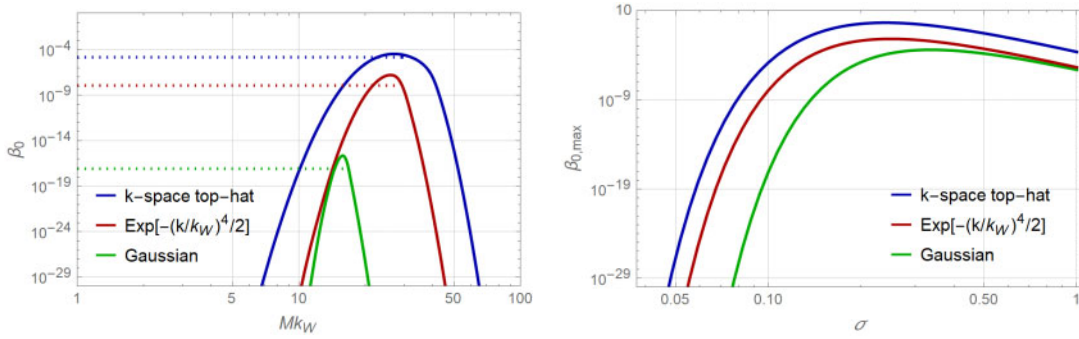

Fig. 3. PBH mass spectrum (left) and $\beta_{0,\text{max}}^{\text{approx}}$ as a function of σ (right) for the flat power spectrum with each window function. In the left panel we set $\sigma = 0.1$ and the dotted horizontal lines show the corresponding values of $\beta_{0,\text{max}}^{\text{approx}}$.

$$W_{k\text{TH}}(k/k_W) = \Theta(k_W - k), \tag{41}$$

where we note that W_1 is the standard Gaussian window function.[6] For each window function, we can calculate the PBH mass spectrum with a fixed value of k_W following the procedure presented in the previous section. The results are shown in Fig. 3, where it can be seen that the result significantly depends on the window function. For the overall mass spectrum, taking the envelope curve of the mass spectra for all values of k_W, we obtain a flat mass spectrum with the amplitude given by the maximum value in the plot. Therefore, the k-space tophat window function gives the largest abundance, as expected. This behavior is contrary to the case of the conventional Press–Schechter (PS) formalism where the Gaussian window function gives a larger abundance than the k-space tophat window (see Appendix B and Ref. [8]). The σ-dependence of $\beta_{0,\text{max}}^{\text{approx}}$, which gives an order-of-magnitude estimate for the maximum value of the mass spectrum, is also shown in Fig. 3.

---

[6] The real-space tophat window function leads divergent gradient moments for the scale-invariant flat spectrum, so that practically we cannot use it.

6. Summary and discussion

We have improved the procedure proposed in Ref. [25] so that we can decouple the larger-scale environmental effect, which is irrelevant to the PBH formation. Thus, we can eliminate the redundant variance due to the environmental effect, and obtain a narrower mass spectrum than Ref. [25]. This new procedure also allows us to straightforwardly implement a window function and calculate the PBH abundance for an arbitrary power spectrum of the curvature perturbation. For a sufficiently narrow power spectrum, the PBH mass spectrum results in the case without the window function irrespective of the choice of the window function. That is, there is no window function dependence for a sufficiently narrow spectrum in our procedure.

It should be noted that Ref. [26] attempted to estimate PBH abundance for a broad spectrum without a window function. The results in Ref. [26] show a significant enhancement of the mass spectrum in the large-mass region compared with our results. Although the reason for this discrepancy should be further investigated in the future, we discuss it in Appendix C.

The PBH abundance for the scale-invariant flat power spectrum has been calculated in Sect. 5 as an example. The result largely depends on the choice of the window function. Nevertheless, we found that the k-space tophat window function has the minimum required property. Specifically, it minimizes the extra reduction of the mass spectrum due to the window function. When one estimates PBH abundance without any concrete physical smoothing process, the choice of the k-space tophat window function would be the best in our procedure. Finally, we emphasize that our procedure makes it possible to calculate the PBH mass spectrum for an arbitrary power spectrum by using a plausible PBH formation criterion with the nonlinear relation taken into account.

Appendix A.   Random Gaussian distribution of ζ

Due to the random Gaussian assumption, the probability distribution of any set of linear combinations of the variable $\zeta(x_i)$ is given by a multidimensional Gaussian probability distribution [28,38],

$$P(V_I)d^n V_I = (2\pi)^{-n/2} |\det \mathcal{M}|^{-1/2} \exp\left[-\frac{1}{2} V_I \left(\mathcal{M}^{-1}\right)^{IJ} V_J\right] d^n V, \qquad (A.1)$$

where the components of the matrix $\mathcal{M}$ are given by the correlation $\langle V_I V_J \rangle$ defined by

$$\langle V_I V_J \rangle := \int \frac{d\boldsymbol{k}}{(2\pi)^3} \frac{d\boldsymbol{k}'}{(2\pi)^3} \langle \tilde{V}_I^*(\boldsymbol{k}) \tilde{V}_J(\boldsymbol{k}') \rangle, \qquad (A.2)$$

with $\tilde{V}_I(\boldsymbol{k}) = \int d^3 x V_I(\boldsymbol{x}) e^{i\boldsymbol{k}\boldsymbol{x}}$.

The nonzero correlations between two of $\nu = -\zeta/\sigma_0$, $\xi = \Delta\zeta/\sigma_2$, and $\omega = -\Delta\Delta\zeta/\sigma_4$ are given by

$$\langle \nu\nu \rangle = \langle \xi\xi \rangle = \langle \omega\omega \rangle = 1, \qquad (A.3)$$

$$\langle \nu\xi \rangle = \gamma_1 := \sigma_1^2/(\sigma_0\sigma_2), \qquad (A.4)$$

$$\langle \nu\omega \rangle = \gamma_2 := \sigma_2^2/(\sigma_0\sigma_4), \tag{A.5}$$

$$\langle \xi\omega \rangle = \gamma_3 := \sigma_3^2/(\sigma_2\sigma_4). \tag{A.6}$$

Then, the probability distribution function for these variables is given by

$$P(\nu,\xi,\omega) = (2\pi)^{-3/2}\,|D|^{-1/2}\exp\Bigg[-\frac{1}{2D}\Big\{(1-\gamma_3^2)\nu^2 + (1-\gamma_2^2)\xi^2 + (1-\gamma_1^2)\omega^2$$
$$-\,2(\gamma_1-\gamma_2\gamma_3)\nu\xi - 2(\gamma_2-\gamma_3\gamma_1)\omega\nu - 2(\gamma_3-\gamma_1\gamma_2)\xi\omega\Big\}\Bigg], \tag{A.7}$$

where

$$D = \det\mathcal{M} = 1 - \gamma_1^2 - \gamma_2^2 - \gamma_3^2 + 2\gamma_1\gamma_2\gamma_3 \tag{A.8}$$

with

$$\mathcal{M} = \begin{pmatrix} 1 & \gamma_1 & \gamma_2 \\ \gamma_1 & 1 & \gamma_3 \\ \gamma_2 & \gamma_3 & 1 \end{pmatrix}. \tag{A.9}$$

We re-express the probability P as a probability distribution function $\tilde{P}$ of ζ_0, μ_2, and $k_\bullet$:

$$\tilde{P}(\zeta_0,\mu_2,k_\bullet)d\zeta_0 d\mu_2 dk_\bullet = P(\nu,\xi,\omega)d\nu d\xi d\omega = \frac{2\mu_2 k_\bullet}{\sigma_0\sigma_2\sigma_4}P\left(\frac{\zeta_0}{\sigma_0},\frac{\mu_2}{\sigma_2},\frac{\mu_2 k_\bullet^2}{\sigma_4}\right)d\zeta_0 d\mu_2 dk_\bullet. \tag{A.10}$$

Then, the conditional probability $p(\zeta_0)$ with fixed μ_2 and $k_\bullet$ is given by

$$p(\zeta_0) = \left(\frac{1-\gamma_3^2}{2\pi D\sigma_0^2}\right)^{1/2}\exp\left[-\frac{1-\gamma_3^2}{2D\sigma_0^2}\left(\zeta_0-\bar{\zeta}_0\right)^2\right] = \left(\frac{1-\gamma_3^2}{2\pi D\sigma_0^2}\right)^{1/2}\exp\left[-\frac{1-\gamma_3^2}{2D\sigma_0^2}\zeta_\infty^2\right], \tag{A.11}$$

where

$$\bar{\zeta}_0 = -\mu_2\frac{\left(\sigma_1^2\sigma_4^2-\sigma_2^2\sigma_3^2\right)+\left(\sigma_2^4-\sigma_1^2\sigma_3^2\right)k_\bullet^2}{\sigma_2^2\sigma_4^2-\sigma_3^4}. \tag{A.12}$$

Appendix B.　Estimation and window function dependence in the Press–Schechter formalism

For a comparison, we review a conventional estimate of the fraction of PBHs based on the PS formalism. In the conventional formalism, the scale dependence is introduced by a window function $W(k/k_M)$, where

$$k_M = k_{\rm eq}(M_{\rm eq}/M)^{1/2}. \tag{B.1}$$

Then, each gradient moment is replaced by the following expression:

$$\hat{\sigma}_n(k_M)^2 = \int \frac{dk}{k}k^{2n}\mathcal{P}(k)W(k/k_M)^2. \tag{B.2}$$
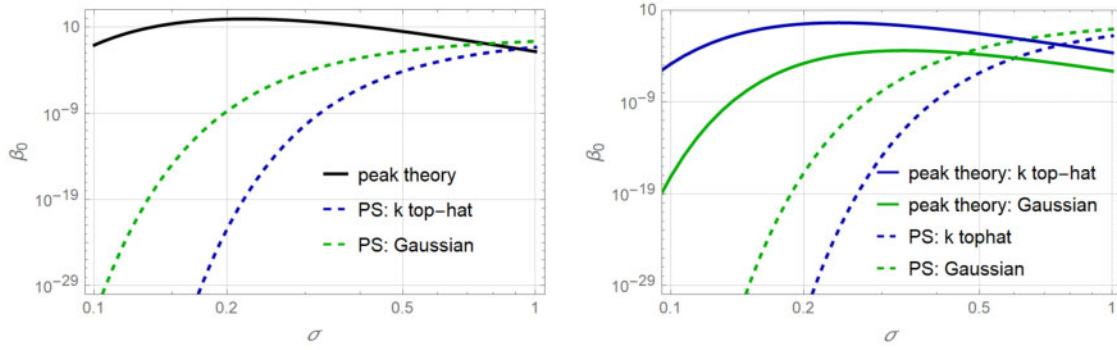
Fig. B.1. The window function dependencies of the PS formalism and our procedure are shown for the monochromatic spectrum (left) and the flat spectrum (right). The solid lines and dashed lines show the results for our procedure based on the peak theory and for the PS formalism, respectively. In the left panel, the values for the PS formalism are given by Eq. (B.6) with $k_0 = k_M$, and the value in our procedure is depicted as a single solid line because the fraction of PBH does not depend on the window function in our procedure.

The conventional estimate starts from the following Gaussian distribution assumption for the density perturbation $\bar{\delta}$:

$$P_\delta(\bar{\delta})d\bar{\delta} = \frac{1}{\sqrt{2\pi}\sigma_\delta} \exp\left(-\frac{1}{2}\frac{\bar{\delta}^2}{\sigma_\delta^2}\right) d\bar{\delta}, \tag{B.3}$$

where σ_δ is given by the coarse-grained density contrast,

$$\sigma_\delta(k_M) = \frac{4}{9}\frac{\hat{\sigma}_2(k_M)}{k_M^2}. \tag{B.4}$$

Here, for simplicity, we use the same numerical value of $\delta_{\rm th}$ as in our approach; in other words, we assume that the volume average of the density perturbation obeys the Gaussian probability distribution given by Eq. (B.3) with the coarse-grained density contrast of Eq. (B.4) in the PS formalism. This Gaussian distribution and the dispersion are motivated by the linear relation between ζ and δ. The fraction $\beta_0^{\rm PS}$ is then evaluated (see, e.g., Ref. [39]) as

$$\beta_0^{\rm PS}(M) = 2\alpha \int_{\delta_{\rm th}}^\infty d\bar{\delta} P_\delta(\bar{\delta}) = \alpha\,{\rm erfc}\left(\frac{\delta_{\rm th}}{\sqrt{2}\,\sigma_\delta(k_M)}\right) = \alpha\,{\rm erfc}\left(\frac{9}{4}\frac{\delta_{\rm th}k_M^2}{\sqrt{2}\hat{\sigma}_2(k_M)}\right). \tag{B.5}$$

Let us check the window function dependence in the PS formalism for the cases of the monochromatic spectrum $\mathcal{P}(k) = \sigma^2 k_0 \delta(k - k_0)$ and the flat spectrum $\mathcal{P}(k) = \sigma^2$. For the monochromatic spectrum, the fraction $\beta_{0,{\rm mono}}^{\rm PS}$ is given by

$$\beta_{0,{\rm mono}}^{\rm PS} = {\rm erfc}\left(\frac{9}{4}\frac{\delta_{\rm th}k_M^2}{\sqrt{2}\sigma k_0^2 W(k_0/k_M)}\right). \tag{B.6}$$

From this expression, the existence and significance of the window function dependence is clear (see the left panel of Fig. B.1). On the other hand, as stated in the first paragraph of Sect. 5, for a narrow power spectrum there is essentially no window function dependence in our procedure. In particular, for the monochromatic spectrum case the fraction reduces to the result given in Ref. [25] for an arbitrary window function satisfying the properties listed in the same paragraph.

For the flat spectrum, the value of the second gradient moment is given by $\sigma k_M^2/\sqrt{2}$ and $\sigma k_M^2/2$ for the Gaussian and k-space tophat window functions, respectively. Therefore, in the PS formalism the abundance is larger for the Gaussian window function, different from our case shown in Fig. 3. In the right panel of Fig. B.1 the window function dependencies in the PS formalism and our procedure are shown. In both cases, the window function dependence is significant at a similar extent.

It should be noted that in the PS formalism the reason for the larger abundance for the Gaussian window is the contribution from the high-k modes through the tail of the Gaussian function. Therefore, it is clear that the longer the tail of the window function, the larger the abundance becomes. Of course, we cannot take the long-tail limit because the window function becomes irrelevant in this limit. Contrary to the PS formalism, in our procedure the sharpest cutoff in the k-space gives the largest abundance, and the extra reduction due to the window function can be minimized in this well-defined limit.

Appendix C.   Discrepancy between our results and Ref. [26]

As noted in Sect. 6, a qualitative difference can be seen between our PBH mass spectrum and that in Ref. [26] in the large-mass region. First, we briefly review the basic idea used in Ref. [26] (see also Ref. [40]).

In order to clearly distinguish the equations which are valid only for spherically symmetric cases from generally valid equations, we use the notation $\overset{\circ}{=}$ for equality with spherical symmetry. Let us start with the relation between the nonlinear volume-averaged density perturbation $\bar{\delta}$, the compaction function $\mathcal{C}$, and the curvature perturbation [22]:

$$\bar{\delta} \overset{\circ}{=} 2\mathcal{C} \overset{\circ}{=} \frac{2\delta M}{R} \overset{\circ}{=} -\frac{2}{3} r_R \zeta_R' [2 + r_R \zeta_R'], \tag{C.1}$$

where r_R is a certain radius and the subscript $_R$ denotes the value at $r = r_R$.[7] This equation is valid for super-horizon spherically symmetric perturbations. We may define δ_1, which is linearly related to ζ, as follows:

$$\delta_1 \overset{\circ}{=} -\frac{4}{3} r_R \zeta_R'. \tag{C.2}$$

Then we obtain

$$\bar{\delta} \overset{\circ}{=} \delta_1 - \frac{3}{8}\delta_1^2. \tag{C.3}$$

The linear density perturbation δ_1 should be compared with δ_R defined in Eq. (9) of Ref. [26] as follows:

$$\delta_R(r_R) = \frac{3}{4\pi r_R^3} \int d^3x \frac{\delta\rho}{\rho} \theta(r_R - |\vec{x} - \vec{x}_0|), \tag{C.4}$$

where θ is the Heaviside step function, which effectively acts as the real-space tophat window function. We note that this expression is defined not only for spherically symmetric perturbations

---

[7] r_R corresponds to R in Ref. [26].

but for general ones. Using the linear relation

$$\frac{\delta\rho}{\rho} = -\frac{4}{9}\frac{1}{a^2H^2}\Delta\zeta \overset{\circ}{=} -\frac{4}{9}\frac{1}{a^2H^2}\frac{1}{r^2}\partial_r(r^2\partial_r\zeta) \tag{C.5}$$

in a spherically symmetric case, we can find [40]

$$\delta_R(r_R) \overset{\circ}{=} \frac{4}{3r_R}\int_0^{r_R} drr^2\left(\zeta'' + \frac{2}{r}\zeta'\right) \overset{\circ}{=} -\frac{4}{3}r_R\zeta_R' \overset{\circ}{=} \delta_l \tag{C.6}$$

at the horizon entry time defined by $r_R = 1/(aH)$.

In Ref. [26], the relation with spherical symmetry $2\mathcal{C} = \delta_l - \frac{3}{8}\delta_l^2$ is extended to the general relation $2\mathcal{C} = \delta_R - \frac{3}{8}\delta_R^2$, and the PBH formation criterion for $\mathcal{C}$ is expressed in terms of δ_R and used to estimate PBH abundance. δ_R is equivalent to the linear density perturbation with the real-space tophat window function. However, it should be noted that the real-space tophat window function is naturally introduced so that the relation Eq. (C.6) can be satisfied, and not introduced by hand as a window function.

Let us consider the estimation of PBH abundance in the large-mass region where the discrepancy exists. For simplicity, let us focus on a single-scale power spectrum with the typical scale $1/k_0$. First, we note that in Ref. [26] the value of r_R is chosen such that $d\delta_R/dr_R = 0$ and $\mathcal{C}(\vec{x}, r_R)$ takes a maximal value at $\vec{x} = \vec{x}_0$, where $\mathcal{C}$ is regarded as a function of $\vec{x}$ and r_R. The scale of the region relevant to PBH formation is given by r_R, which can be significantly different from $1/k_0$.[8] However, the relevance of the present criterion given in terms of the compaction function $\mathcal{C}$ is not clear for the outer maxima. In Fig. 2 of Ref. [41], the result of a numerical simulation for a spherically symmetric and oscillatory initial profile is shown. The initial profile in the simulation corresponds to the most probable profile for a delta-function power spectrum peaked at $1/k_0$. The most probable profile is given by a peak at the center surrounded by repeated concentric overdense and underdense regions. More precisely, the most probable profile of the curvature perturbation is given by a sinc function, where the compaction function is oscillatory with respect to the distance from the center. We can find that the PBH formation criterion is satisfied for the multiple radii corresponding to the maxima in Fig. 2 of Ref. [41]. The resultant PBH, however, has a mass corresponding to the typical scale $1/k_0$, whereas no PBH of larger mass scales is formed. This result suggests that the present criterion is relevant only for the innermost maximum of the compaction function but not for the outer maxima. If the present criterion is simply applied to not only the innermost but also outer maxima, the abundance of primordial black holes of large-mass scales could be overestimated.

References

[1] Y. B. Zel'dovich and I. D. Novikov, Sov. Ast. **10**, 602 (1967).
[2] S. Hawking, Mon. Not. Roy. Astron. Soc. **152**, 75 (1971).
[3] B. Carr, K. Kohri, Y. Sendouda, and J. Yokoyama, arXiv:2002.12778 [astro-ph.CO] [Search INSPIRE].
[4] B. Carr and F. Kühnel, Annu. Rev. Nucl. Part. Sci. **70**, 355 (2020) [arXiv:2006.02838 [astro-ph.CO]] [Search INSPIRE].
[5] B. P. Abbott et al. [LIGO Scientific and Virgo Collaborations], Phys. Rev. Lett. **116**, 061102 (2016) [arXiv:1602.03837 [gr-qc]] [Search INSPIRE].
[6] M. Sasaki, T. Suyama, T. Tanaka, and S. Yokoyama, Phys. Rev. Lett. **117**, 061101 (2016); **121**, 059901 (2018) [erratum] [arXiv:1603.08338 [astro-ph.CO]] [Search INSPIRE].

---

[8] In our procedure, the relevant scale is $r_{\rm m} \sim 1/k_0$.

[7]   V. De Luca, G. Franciolini, A. Kehagias, M. Peloso, A. Riottoa, and C. Ünal, J. Cosmol. Astropart. Phys. **1907**, 048 (2019) [arXiv:1904.00970 [astro-ph.CO]] [Search INSPIRE].

[8]   K. Ando, K. Inomata, and M. Kawasaki, Phys. Rev. D **97**, 103528 (2018) [arXiv:1802.06393 [astro-ph.CO]] [Search INSPIRE].

[9]   S. Young, Int. J. Mod. Phys. D **29**, 2030002 (2020) [arXiv:1905.01230 [astro-ph.CO]] [Search INSPIRE].

[10] K. Tokeshi, K. Inomata, and J. Yokoyama, arXiv:2005.07153 [astro-ph.CO] [Search INSPIRE].

[11] B. J. Carr, Astrophys. J. **201**, 1 (1975).

[12] D. K. Nadezhin, I. D. Novikov, and A. G. Polnarev, Sov. Ast. **22**, 129 (1978).

[13] I. D. Novikov and A. G. Polnarev, Sov. Ast. **24**, 147 (1980).

[14] M. Shibata and M. Sasaki, Phys. Rev. D **60**, 084002 (1999) [arXiv:gr-qc/9905064] [Search INSPIRE].

[15] J. C. Niemeyer and K. Jedamzik, Phys. Rev. D **59**, 124013 (1999) [arXiv:astro-ph/9901292] [Search INSPIRE].

[16] I. Musco, J. C. Miller, and L. Rezzolla, Class. Quantum Grav. **22**, 1405 (2005) [arXiv:gr-qc/0412063] [Search INSPIRE].

[17] A. G. Polnarev and I. Musco, Class. Quantum Grav. **24**, 1405 (2007) [arXiv:gr-qc/0605122] [Search INSPIRE].

[18] I. Musco, J. C. Miller, and A. G. Polnarev, Class. Quantum Grav. **26**, 235001 (2009) [arXiv:0811.1452 [gr-qc]] [Search INSPIRE].

[19] A. G. Polnarev, T. Nakama, and J. Yokoyama, J. Cosmol. Astropart. Phys. **1209**, 027 (2012) [arXiv:1204.6601 [gr-qc]] [Search INSPIRE].

[20] T. Nakama, T. Harada, A. G. Polnarev, and J. Yokoyama, J. Cosmol. Astropart. Phys. **1401**, 037 (2014) [arXiv:1310.3007 [gr-qc]] [Search INSPIRE].

[21] T. Harada, C.-M. Yoo, and K. Kohri, Phys. Rev. D **88**, 084051 (2013); **89**, 029903 (2014) [erratum] [arXiv:1309.4201 [astro-ph.CO]] [Search INSPIRE].

[22] T. Harada, C.-M. Yoo, T. Nakama, and Y. Koga, Phys. Rev. D **91**, 084057 (2015) [arXiv:1503.03934 [gr-qc]] [Search INSPIRE].

[23] A. Escrivà, C. Germani, and R. K. Sheth, Phys. Rev. D **101**, 044022 (2020) [arXiv:1907.13311 [gr-qc]] [Search INSPIRE].

[24] A. Escrivà, C. Germani, and R. K. Sheth, arXiv:2007.05564 [gr-qc] [Search INSPIRE].

[25] C.-M. Yoo, T. Harada, J. Garriga, and K. Kohri, Prog. Theor. Exp. Phys. **2018**, 123E01 (2018) [arXiv:1805.03946 [astro-ph.CO]] [Search INSPIRE].

[26] C. Germani and R. K. Sheth, Phys. Rev. D **101**, 063520 (2020) [arXiv:1912.07072 [astro-ph.CO]] [Search INSPIRE].

[27] T. Suyama and S. Yokoyama, Prog. Theor. Exp. Phys. **2020**, 023E03 (2020) [arXiv:1912.04687 [astro-ph.CO]] [Search INSPIRE].

[28] J. M. Bardeen, J. R. Bond, N. Kaiser, and A. S. Szalay, Astrophys. J. **304**, 15 (1986).

[29] I. Musco and J. C. Miller, Class. Quantum Grav. **30**, 145009 (2013) [arXiv:1201.2379 [gr-qc]] [Search INSPIRE].

[30] C.-M. Yoo, J.-O. Gong, and S. Yokoyama, J. Cosmol. Astropart. Phys. **1909**, 033 (2019) [arXiv:1906.06790 [astro-ph.CO]] [Search INSPIRE].

[31] M. W. Choptuik, Phys. Rev. Lett. **70**, 9 (1993).

[32] T. Koike, T. Hara, and S. Adachi, Phys. Rev. Lett. **74**, 5170 (1995) [arXiv:gr-qc/9503007] [Search INSPIRE].

[33] J. C. Niemeyer and K. Jedamzik, Phys. Rev. Lett. **80**, 5481 (1998) [arXiv:astro-ph/9709072] [Search INSPIRE].

[34] J. Yokoyama, Phys. Rev. D **58**, 107502 (1998) [arXiv:gr-qc/9804041] [Search INSPIRE].

[35] A. M. Green and A. R. Liddle, Phys. Rev. D **60**, 063509 (1999) [arXiv:astro-ph/9901268] [Search INSPIRE].

[36] F. Kühnel, C. Rampf, and M. Sandstad, Eur. Phys. J. C **76**, 93 (2016) [arXiv:1512.00488 [astro-ph.CO]] [Search INSPIRE].

[37] C. Germani and I. Musco, Phys. Rev. Lett. **122**, 141302 (2019) [arXiv:1805.04087 [astro-ph.CO]] [Search INSPIRE].

[38] A. G. Doroshkevich, Astrofiz. **6**, 581 (1970).

[39] B. Carr, F. Kühnel, and M. Sandstad, Phys. Rev. D **94**, 083504 (2016) [arXiv:1607.06077 [astro-ph.CO]] [Search INSPIRE].

[40] S. Young, I. Musco, and C. T. Byrnes, J. Cosmol. Astropart. Phys. **1911**, 012 (2019) [arXiv:1904.00984 [astro-ph.CO]] [Search INSPIRE].

[41] V. Atal, J. Cid, A. Escrivà, and J. Garriga, J. Cosmol. Astropart. Phys. **2005**, 022 (2020) [arXiv:1908.11357 [astro-ph.CO]] [Search INSPIRE].